Pakistan Veterinary Journal

ISSN: 0253-8318 (PRINT), 2074-7764 (ONLINE)
DOI: 10.29261/pakvetj/2025.306

RESEARCH ARTICLE

Synthesis of Silver Nanoparticles Using *Tamarindus indica* Leaf Extract: Antioxidant, Antidiabetic Potential and Expression of Diabetes Associated Genes (*TCF7L2/KCNJ11*) in Mice

Sadia Iqbal[1], Farzana Rashid[1]*, Saima Sharif[1], Iqra Noshair[1], Abdullah Etezaz[2], Shagufta Naz[1] and Fakhar-un-Nisa Yunus[1]

[1]Department of Zoology, Faculty of Natural Sciences, Lahore College for Women University, Lahore 54000, Pakistan; [2]Institute of Microbiology, University of Agriculture, Faisalabad, Pakistan
*Corresponding author: dr.farzanarashid@gmail.com

ARTICLE HISTORY (25-909)

Received: September 27, 2025
Revised: October 30, 2025
Accepted: November 03, 2025
Published online: December 02, 2025

Key words:
Antidiabetic
Antioxidant
Silver nanoparticles
Tamarindus indica

ABSTRACT

Nanotechnology has gained considerable attention in diabetic research to enhance therapeutic potential compared to conventional drug therapies. In the present study, silver nanoparticles (AgNPs) were synthesized using *Tamarindus indica* (*T. indica*) leaf extract and characterized through UV–Vis, FTIR, SEM, EDX and XRD analyses, to confirm size and crystalline structure, the average crystallite size of AgNPs had calculated to be around 15–40 nm. The antioxidant potential of both the *T. indica* leaf extract and the synthesized AgNPs (20, 40, 60, 80 and 100µg/mL) were evaluated separately using the DPPH radical scavenging assay. The antidiabetic efficacy of these nanoparticles evaluated in alloxan-induced diabetic mice, 90 male albino mice were used in this study 10 of them were served as control and 80 as the experimental groups. body weight and Blood glucose level were measured with different time intervals over a period of 21 days. Treatment of mice with high-dose AgNPs (100mg/kg) resulted in marked decrease in blood glucose level and increase in body weight. The findings revealed that AgNPs exhibited significant radical scavenging activity (IC_{50}=53.6 µg/mL) compared to the extract (IC_{50}=82.2 µg/mL) standard. The results indicated upregulation of *KCNJ11* and *TCF7L2* genes in diabetic mice, which were restored to normal by treatment with AgNPs. Significant restoration noted in hematological parameters with treatment groups. Histological analysis of pancreas further demonstrated tissue regeneration same as in control group. Overall, the green synthesized AgNPs exhibited strong antidiabetic and antioxidant activity in diabetic mice.

To Cite This Article: Iqbal S, Rashid F, Sharif S, Noshair I, Etezaz A, Naz S and Yunus FN, 2025. Synthesis of silver nanoparticles using *Tamarindus indica* leaf extract: antioxidant, antidiabetic potential and expression of diabetes associated genes (*TCF7L2/KCNJ11*) in mice. Pak Vet J. http://dx.doi.org/10.29261/pakvetj/2025.306

INTRODUCTION

Nanotechnology has rapidly developed into a vital research domain in recent years, particularly in healthcare. Nanoparticles (NPs) are even more biocompatible than conventional therapeutics, and this also contributes to drug efficacy with minimal toxicity. Nanomedicine revolutionized the field of medicine with its comprehensive applications. Silver nanoparticles (AgNPs) have certain characteristics such as high electrical conductivity and chemical stability which make them beneficial in antibacterial, antifungal, antidiabetic, anticancer and anti-inflammatory activities (Saratale *et al*., 2018). Metal nanoparticles are rapidly researched for numerous scientific and medical applications, including drug delivery, molecular imaging (Sabapathi *et al*., 2023).

Metallic nanoparticles can be produced using various biological systems such as plants, bacteria, fungi, and yeast. Among these, plant-based synthesis is particularly advantageous because it is eco-friendly, scalable, and cost-effective, offering a sustainable alternative to conventional chemical methods (Chopra *et al*., 2022; Begum *et al*., 2022).

Green synthesis of AgNPs from plant or fruit extracts became important in the fields of nanomedicine because of the presence of safe, effective and sustainable therapeutic modalities. Plant-based AgNPs exhibit robust antimicrobial antioxidant and anti-inflammatory activities (Rahuman *et al*., 2022). *Tamarindus indica* (*T. indica*), a monotypic genus of family Leguminosae, is a multipurpose Indian tropical tree and is referred to as tamarind. It is naturally known for its antistress and antidiabetic activities (Garg *et*

al., 2018) and contains phytochemicals such as alkaloids, tannins, saponins, glycosides, flavonoids, anthraquinones, terpenoids, phenols. *T. indica* has medicinal uses such as antiasthmatic, antidiabetic, anticancer and antiulcer activities (Komutarin *et al*., 2004; Kuru, 2014).

Diabetes mellitus (DM) is a chronic metabolic disorder because of the failure in the secretion of insulin by pancreatic β-cells, One of the major cause of diabetes is oxidative stress, resulting from excessive production of Reactive Oxygen Species (ROS) induced by high glucose and fatty acid levels (Menati *et al*., 2020).

The apoptosis of pancreatic β-cells, triggered by oxidative stress, is considered the primary cause of insulin deficiency in diabetic patients (Rodrigues *et al*., 2014; Banerjee *et al*., 2017). AgNPs have been reported to enhance insulin secretion in response to glucose, possibly through the inhibition of dipeptidyl peptidase IV (Elumalai *et al*., 2017). It has been observed that medicinal plants and spices offer natural antioxidants and antidiabetic compounds that improve pancreatic function, providing affordable, biocompatible, and low-toxicity alternatives (Jaffar *et al*., 2020).

KCNJ11 and *TCF7L2* gene are the most influential genetic factors in the onset of DM (Li *et al*., 2018; Barroso *et al.,* 2003). Previous research has not investigated how the plant-mediated AgNPs effect on *KCNJ11* and *TCF7L2* genes associated with diabetes in mice. In order to fill this gap, AgNPs synthesized by *T. indica* leaf extract were used to find out effect on *KCNJ11* and *TCF7L2* in DM mice.

MATERIALS AND METHODS

Ethical Statement: The study followed international ethical guidelines for animal use and approved by the Ethical Committee, Faculty of Science and Technology, LCWU, Lahore, Pakistan (Ref. No. Zoo/LCWU/101, dated: 28-06-2024).

Collection and Processing of Plant Extract: Fresh *T. indica* leaves had been collected from the Garden of Bagh-e-Jinnah, Lahore. Leaves thoroughly washed with distilled water and air-dried. Once dried, they were ground into a fine powder. To prepare the extract, 10 g of powdered leaves were mixed with 100 mL of distilled water and heated on hot plate at 100 °C with continuous stirring. Once cooled, the mixture centrifuged at 4000 rpm for 15 minutes, and the supernatant passed through Whatman No. 1 filter paper. The filtrate (extract) obtained was then preserved for subsequent use.

Synthesis of *T. indica*-Mediated AgNPs: One mM silver nitrate ($AgNO_3$) solution prepared in distilled water, to which 10mL of *T. indica* filtrate (extract) added to facilitate the reduction of silver ions. The reaction mixture (90 mL of 1 mM $AgNO_3$ with 10 mL extract) heated at 100 °C with constant stirring until a visible brownish-yellow appeared within 15–20 minutes (Asimuddin *et al*., 2020). The solution left to stand for 24 hrs (hours), then centrifuged at 4000 rpm for 15 minutes. The obtained pellet collected and stored for subsequent experimental analyses (Fig. 1).

Characterization of *T. indica* Conjugated AgNPs

UV–Vis Spectroscopic Analysis: The absorption spectra of *T. indica* extract and synthesized AgNPs were recorded in the range of 100–800 nm using a UV spectrophotometer (UV-2800 Hitachi) with a 1 cm path length.

Fourier Transform Infrared Spectroscopy (FTIR) Analysis: FTIR analysis performed using a Bruker Alpha Platinum ATR to identify functional groups in *T. indica* extract and silver nanoparticles. The shifting of peaks confirmed the interaction between the plant extract and silver sol–gel, as well as the reduction process.

Scanning Electron Microscopy (SEM), Energy Dispersive X-ray Spectroscopy (EDX) and X-ray Diffraction (XRD) Analysis: The morphology, size and surface capping of the synthesized AgNPs with *T. indica* extract were examined using a Scanning Electron Microscope (Nova NANOSEM 450). SEM images provided insight into the size and shape of NPs. EDX analysis performed to evaluate the elemental composition of the synthesized NPs.

XRD analysis performed to assess whether the synthesized AgNPs exhibited a crystalline or amorphous structure.

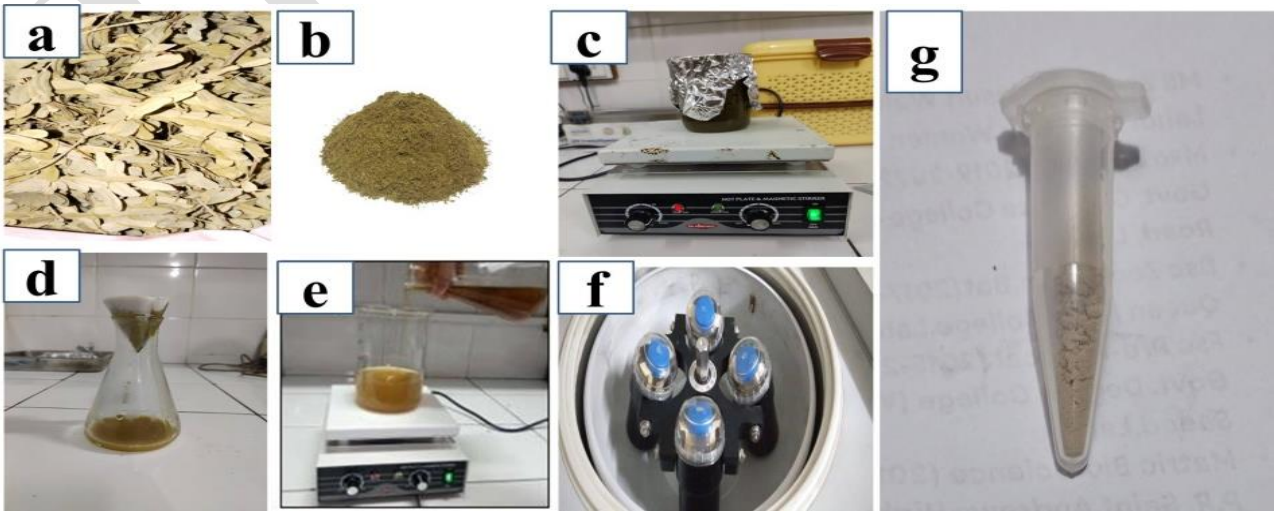

Fig. 1: Green synthesis of *T. indica* conjugated AgNPs. A=*T. indica* leaf; B=leaf powder; C=preparation of extract; D=filtration; E=addition of $AgNO_3$ into filtrate; F=centrifugation; G=Pellet after centrifugation.

Antioxidant Activity: L-ascorbic acid, a well-known antioxidant used as a reference to evaluate the antioxidant potential of the NPs. The free radical scavenging activity of *T. indica* leaf extract and AgNPs assessed using the 2,2-Diphenyl-1-picrylhydrazyl **(**DPPH) (Tahir *et al*., 2023). The absorbance of reaction mixture consisting of 1 mM DPPH solution and 1 mM methanol with varying concentrations of the extract and AgNPs (20, 40, 60, 80 and 100 µg/mL) was measured at 517 nm using a spectrophotometer (UV-1700, Shimadzu, Kyoto, Japan). The experiment was performed in triplicates.

$$\textit{Calculation}\ \%\ \text{scavenging activity} = \frac{\text{Ac} - \text{As}}{\text{Ac}} \times 100$$

Ac denotes the absorbance of the control, while As refers to the absorbance of the experimental sample.

Antidiabetic activity of *T. indica* Conjugated AgNPs

Animal selection and care: The study conducted in the animal house facility at LCWU, Lahore. Ninety (90) male albino mice (weighing 35-40 g and approximately 8 weeks) were obtained from the University of Veterinary and Animal Sciences (UVAS), Lahore. The animals were acclimatized in cages for one week and were maintained on standard laboratory conditions.

Induction of Diabetes in Mice: Animals were categorized into two major groups: control (n=10) and experimental (n=80). Diabetes induced in experimental animals by IP injection of alloxan monohydrate at a dose of 150 mg/kg body weight. To prevent hypoglycemic shock, the animals were provided with 10% glucose solution for 24 hrs following the injection. Blood glucose levels were assessed 72 hrs post-injection. The animals with blood glucose levels ≥ 220 mg/dL were considered diabetic.

Experimental Design: For the antidiabetic study, the animals were divided into eight subgroups, each with ten male mice. The control group received saline solution, whereas the experimental groups given treatments for 21 days. Group I: Control; Group II: Diabetic non-treated group; Group III: Diabetic+Extract (100mg/kg); Group IV: Diabetic+Insulin (100 IU/mL) ; Group V: Diabetic+Low dose of AgNPs (50mg/kg); Group VI: Diabetic+High dose of AgNPs (100mg/kg); Group VII: Diabetic+Low dose of AgNPs (50mg/kg)+Insulin (100IU/mL); Group VIII: Diabetic+High dose of AgNPs (100mg/kg)+Insulin (100IU/mL); Group IX: Diabetic+Insulin (100 IU/mL)+Extract (100mg/kg). Fasting blood glucose levels and body weight were recorded on day 0, 7, 14 and 21.

Animal Treatment and Sample Collection: Mice were treated for 21 days, after which they were fasted for 12 hrs and anesthetized with chloroform following anesthesia blood and pancreatic tissue samples were collected. Blood samples were collected in serum separation tubes containing a gel barrier and centrifuged after 30 minutes at 4000 rpm for 15 minutes to obtain serum. Pancreatic tissues were fixed in 10% formalin solution for histological examination.

RNA Isolation and cDNA Synthesis: To evaluate gene expression, blood samples had been processed for mRNA isolation within 2–4 hrs after collection (Rio *et al*., 2010). The concentration and purity of mRNA were determined by NanoDrop spectrophotometer (Multiskan SkyHigh Microplate, U.K). Subsequently, mRNA reverse transcribed into cDNA with the Maxima R First Strand cDNA Synthesis Kit (Thermo Scientific, CAT # K1622) in the thermal cycler (PTC-06, U.K).

Expression Analysis by Real Time PCR: Real-time PCR carried out using Applied Biosystems StepOne™ Real-Time PCR system (Thermo Fisher Scientific, U.S.). Oligonucleotide primers designed with Primer3 software and their sequences along with optimization conditions (Table 1). Relative expression levels of *KCNJ11* and *TCF7L2* were quantified using the Maxima SYBR Green Master Mix (CAT # K0221). The glyceraldehyde 3-phosphate dehydrogenase (*GAPDH*) gene served as control. The RT-PCR protocol included an initial denaturation at 94°C for 4 minutes, followed by 30 amplification cycles (55°C for 20–30 seconds and 72°C for 45 seconds and a final extension step at 72°C for 5 minutes.

Table 1: Primers used in the study

Genes	Primers	Product Size (bp)	Tm (°C)
KCNJ11	F:TGGGTGGTAACGGCATCTTC	20	61.9
	R: GGTGCAGGTCACTAGGAGC	19	61.7
TCF7L2	F:CACCGACAGTCAAGCAGGAAT	21	54.8
	R: CCACCTTGGCTCTCATCTCTTT	22	54.2

Hematological Analysis: Blood parameters including hemoglobin (Hb), white blood cells (WBCs), red blood cells (RBCs), hematocrit (HCT), mean corpuscular volume (MCV), mean corpuscular hemoglobin (MCH), mean corpuscular hemoglobin concentration (MCHC) and platelets were measured using an automated hematology analyzer (Sysmex KX-21, Kobe, Japan).

Histological Examination: Pancreas tissue sample (3–4 mm thick) were fixed in 10% formalin overnight. The tissues were dehydrated using a graded ethanol series, cleared with xylene and embedded in paraffin wax at 58–60 °C. Tissue sections of 5 µm thickness were prepared using a microtome, which were stained using hematoxylin and eosin (Fischer *et al*., 2018) and then observed under a microscope.

Statistical Analysis: Data are presented as mean±SD and were analyzed with GraphPad Prism (version 9.5.1). Statistical comparisons among groups were conducted using one way ANOVA, followed by a Tukey's multiple comparisons test. Results indicated statistically significant different at * P<0.05; ** P<0.01; *** P<0.001 and **** P<0.0001.

RESULTS

Characterization of AgNPs

UV-Vis Spectral Analysis: UV–Vis analysis displayed a distinct absorption peak between 351–366 nm, confirming the successful formation of *T. indica*-mediated AgNPs (Fig. 2**)**.

Morphology of NPs and Qualitative Analysis: SEM analysis revealed that AgNPs were predominantly crystalline in shape with an average size around 15–40 nm. The plant extract displayed larger clusters and particles whereas the NPs showed minimal aggregation (Fig. 3a, 3b).

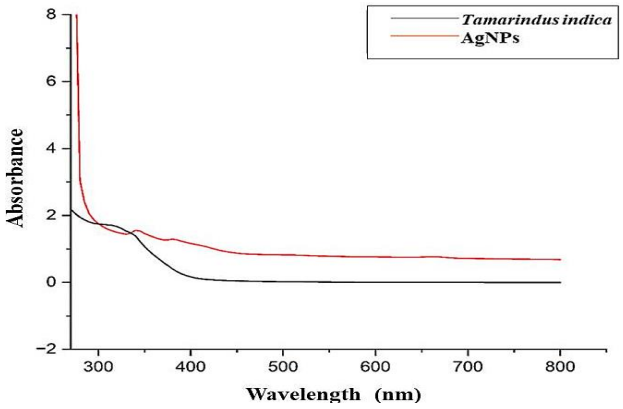

Fig. 2: UV spectral analysis of *T. indica* extract and AgNPs.

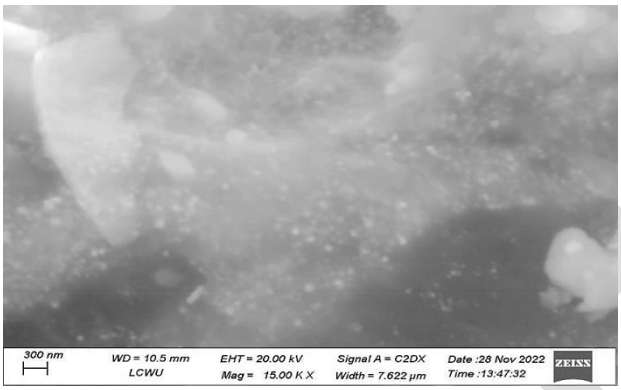

Fig. 3(a): Morphological and surface characterization of the leaf extract.

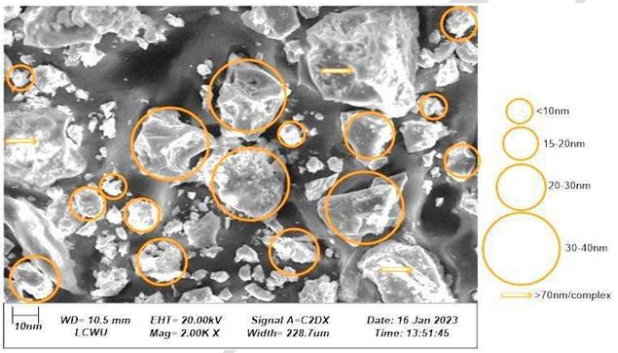

Fig. 3(b): Morphological and surface characterization of the AgNPs.

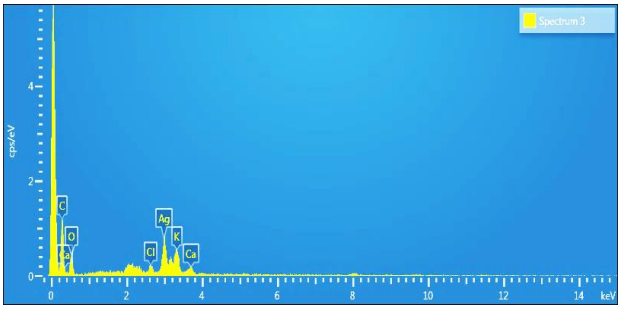

Fig. 3(c): Energy Dispersive X-ray (EDX) analysis of the AgNPs.

Functional Group Analysis Using FTIR: FTIR spectroscopy carried out to identify bioactive compounds in the *T. indica* extract that contributed to the reduction of silver ions. The FTIR spectra of both *T. indica* extract and the synthesized AgNPs were recorded within the wavenumber range of 500–4000 cm^{-1}. The extract showed characteristic peaks at 2401.74 cm^{-1} (O=C=O stretching) and 3184.66 cm^{-1} (N–H stretching). Additional distinct peaks were observed at 2098.23 cm^{-1} (N=N=N stretching), 1622.54 cm^{-1} (C=C stretching), and 1301.23 cm^{-1} (C–N stretching). In contrast, the AgNPs displayed peaks at different wavenumbers, such as 417.53 cm^{-1}, which indicated bond shifts due to NPs formation, and 643.69 cm^{-1}, suggesting potential interactions between the AgNPs and phytochemicals in the plant extract (Fig. 4).

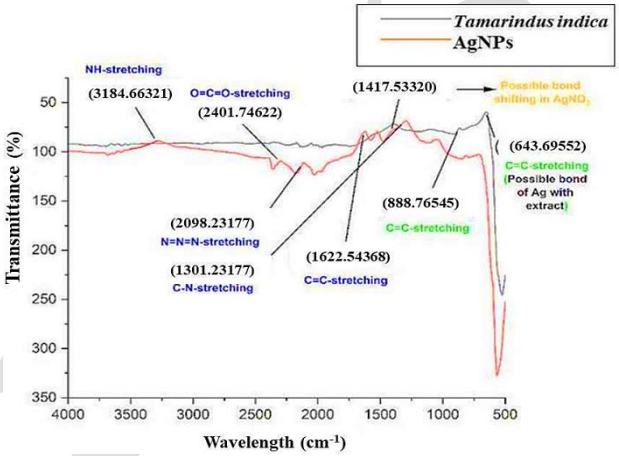

Fig. 4: FTIR-based structural analysis of *T. indica* and AgNPs.

XRD Analysis: XRD analysis revealed distinct peaks of AgNPs at 2θ values of 24.7°, 30.7°, 37.9°, 42.6° and 63.9°. Additionally, the extract exhibited multiple diffraction peaks at 22.1°, 27.4°, 37.9°, 42.6°, 63.2° and 68.7° (Fig. 5).

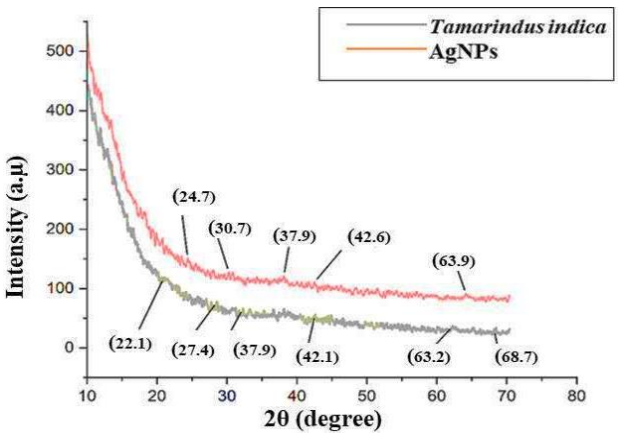

Fig. 5: XRD analysis of the extract and synthesized AgNPs.

Phytochemical Screening: Phytochemical screening of *T. indica* leaf extract indicated the presence of multiple bioactive constituents. The results revealed that the leaves contained alkaloids, terpenoids, glycosides, flavonoids, saponins and tannins (Table 2).

Antioxidant Activity: The findings showed that free radical inhibition was concentration-dependent, with

higher analyte levels producing greater activity (Fig. 6). *T. indica* extract displayed radical scavenging potential comparable to ascorbic acid. In contrast, the AgNPs demonstrated superior scavenging efficiency, with an IC_{50} of 53.6 µg/mL, lower than that of the extract (IC_{50}=82.2 µg/mL) and ascorbic acid (IC_{50}=67.5 µg/mL).

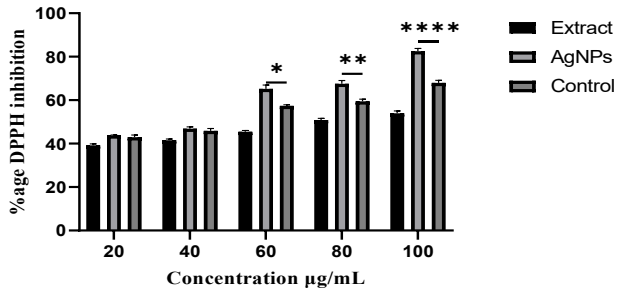

Fig. 6: DPPH radical scavenging activity of *T. indica* extract and synthesized AgNPs shows concentration-dependent antioxidant potential. Asterisks indicate (One-way ANOVA, *P<0.05, **P<0.01, ****P<0.0001) significant difference.

Table 2: Screening of bioactive compounds in the ethanolic extract of *T. indica*

Phytochemical	Result	Indication	Observation
Alkaloids	Orange colored	+	
Terpenoids	Blue- green ring	+	
Glycosides	Green-blue color	+	
Flavonoids	Dark yellow color	+	
Saponins	Froth formation	+	
Tannins	Blue- green color	+	

*(+) indicates presence

In vivo Antidiabetic Activity

Assessment of Body Weight: The body weight of mice monitored on day first, seven, fourteen and twenty-one to evaluate the effects of various treatments (Table 3). A progressive decline in body weight recorded in the diabetic control group (Group II), decreasing from 36.18±0.21 g before induction to 28.67±0.33 g on day 21, confirming the catabolic effect of hyperglycemia. In contrast, all treatment groups showed progressive weight gain compared to diabetic control. The high-dose AgNPs group (Group VI) exhibited the maximum weight gain, increasing from 36.10±0.28 g to 44.67±0.88 g by day 21. Mice treated with AgNPs combined with insulin (Group VIII) also showed a substantial improvement, reaching 39.90±0.10 g at the end of the experiment.

The extract-treated group (Group III) and insulin-treated group (Group IV) demonstrated gradual increases in body weight, reaching 40.33±0.33 g and 39.67±0.28 g, respectively. Similarly, low-dose AgNPs (Group V) and low-dose AgNPs+insulin (Group VII) induced moderate weight recovery, attaining 39.67±0.33 g and 40.33±0.33 g, respectively, by day 21. The high-dose AgNPs alone (Group VI) demonstrated the most pronounced effect on weight gain, followed by combination therapies, whereas the diabetic control group exhibited continuous weight loss throughout the study.

Blood Glucose Level Assessment: The blood glucose levels of all experimental animals were recorded with following the same time intervals as stated earlier to evaluate the antidiabetic effects of treatments (Fig. 7). The diabetic control group (Group II) exhibited a progressive and significant rise in blood glucose levels from 121.7±4.4 mg/dL on Day 0 to 194.7±3.84 mg/dL on Day 21, confirming successful induction of hyperglycemia.

In contrast, all treatment groups demonstrated various degrees of blood glucose reduction compared to diabetic control. The high-dose AgNPs (100 mg/kg; Group VI) exhibited a statistically significant reduction, reaching 114.7±0.88 mg/dL by day 21, approaching near-normal levels (Fig. 8). The high-dose AgNPs+insulin group (Group VIII) also showed statistically significant reduction in blood glucose levels from 115.3±0.33 mg/dL to 122±2.51 mg/dL. Other combination therapies, including insulin+extract (Group IX) and animals administered low-dose AgNPs (50 mg/kg)+insulin (Group VII), resulted in final glucose levels of 120±3.12 mg/dL and 124.7±2.60 mg/dL, respectively. The extract-only group (Group III) and insulin-only group (Group IV) also improved glucose control, ending at 124.7±0.88 mg/dL and 128.7±0.88 mg/dL, respectively. High-dose AgNPs (Group VI) produced the most pronounced glucose-lowering effect, followed by combination therapies, while the diabetic control group continued to exhibit hyperglycemia throughout the study.

Table 3: Impact of various treatments on the body weight of albino mice in antidiabetic activity

Group	Treatment	Body weight (g)				
		Before induction of diabetic	Day 0	Day 7	Day 14	Day 21
I	Control	36.42±0.17	36.50/0.26	36.63/0.31	36.67/0.48	36.80/0.15
II	Diabetic	36.18±0.21	35.83±0.16	33.77±0.23	31.77±0.95	28.67±0.33
III	Diabetic+Extract	37.03±0.34	37.23±0.61	37.93±0.06	39.27±0.73	40.33±0.33
IV	Diabetic+Insulin	35.98±0.31	36.37±0.52	36.97±0.23	38.63±0.36	39.67±0.28
V	Diabetic+Low dose of AgNPs	36.97±0.27	36.73±0.44	37.27±0.37	38.67±0.88	39.67±0.33
VI	Diabetic+High dose of AgNPs	36.10±0.28	36.20±0.40	38±0.57	42.33±0.66	44.67±0.88
VII	Diabetic+Low dose of AgNPs+ Insulin	36.78±0.18	36.77±0.38	37.73±0.58	39.67±0.33	40.33±0.33
VIII	Diabetic+High dose of AgNPs+ Insulin	36.87±0.12	37±0.26	37.17±0.42	39.57±0.29	39.90±0.10
IX	Diabetic+Insulin+Extract	37.13±0.18	37.17±0.266	37.30±0.35	39.97±0.033	40.17+0.166

* All the values are given as Mean ± SD

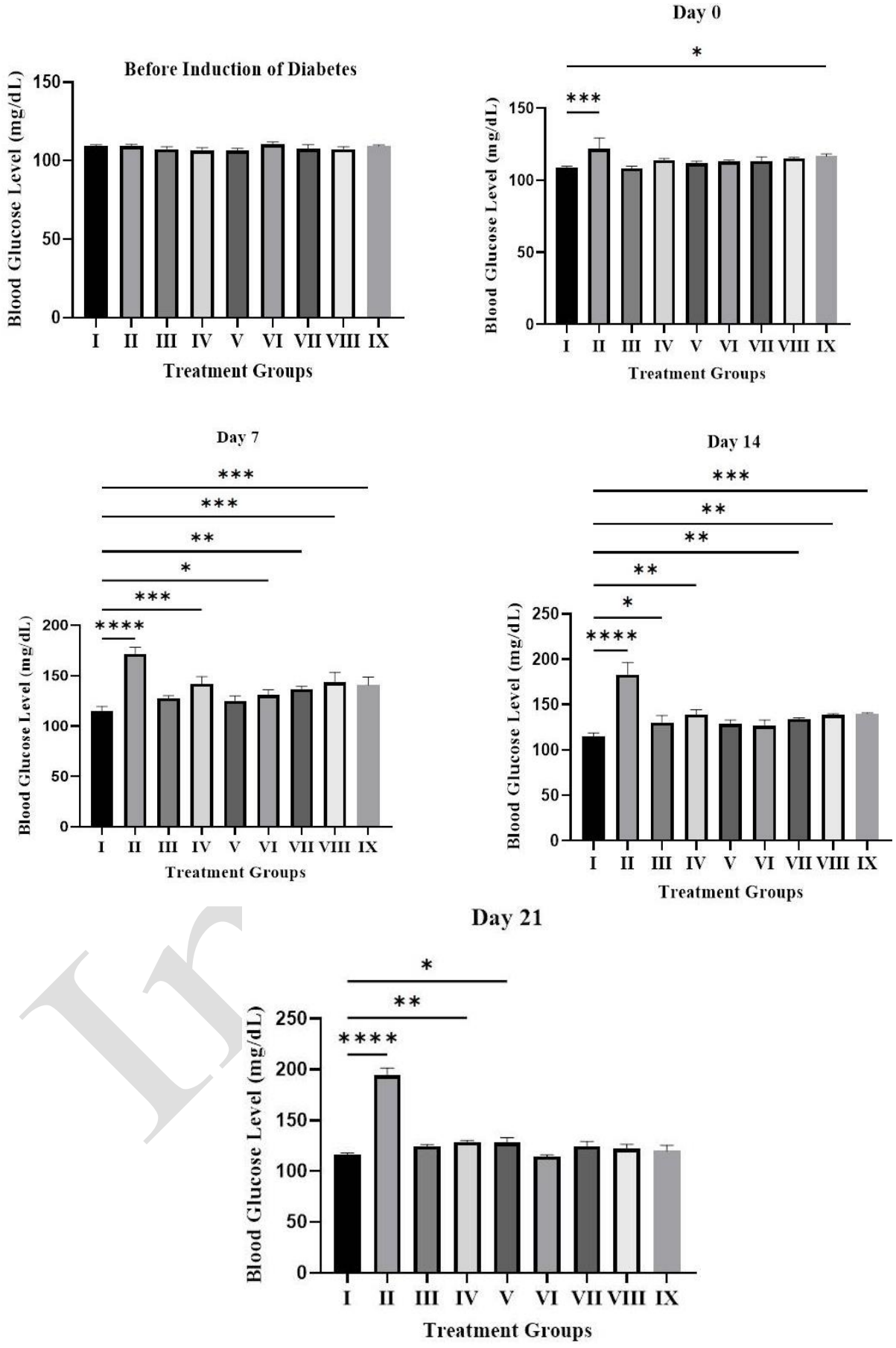

Fig. 7: Blood glucose level before induction of diabetes and from day 0 to 21st of treatment. Asterisks indicate (One-way ANOVA, *P<0.05; **P<0.01,***P<0.001, ****P<0.0001) significant difference. Group I: Control; Group II: Diabetic; Group III: Diabetic+Extract; Group IV: Diabetic+Insulin; Group V: Diabetic+Low dose of AgNPs; Group VI: Diabetic+High dose of AgNPs; Group VII: Diabetic+Low dose of AgNPs+ Insulin; Group VIII: Diabetic+High dose of AgNPs+ Insulin; Group IX: Diabetic +Insulin+ Extract.

***KCNJ11* and *TCF7L2* Gene Expression:** The expression level of *KCNJ11* gene analyzed across different treatment groups (Fig. 8a). A significant upregulation observed in the diabetic group (Group II) compared to the control group (Group I). Treatment with plant extract (Group III), insulin (Group IV), low dose of AgNPs (Group V), high dose of AgNPs (Group VI), and their respective combinations with insulin (Groups VII–IX) did not show a significant difference in *KCNJ11* expression compared to the control group. These results indicate that diabetes markedly elevates *KCNJ11* gene expression, while therapeutic interventions (extract, insulin, AgNPs, and their combinations) tend to normalize its expression toward control levels. The expression profile of the *TCF7L2* gene across different treatment groups is presented in Fig. 8b. A highly significant upregulation observed in the diabetic group (Group II) compared to the control group (Group I). Treatment with plant extract (Group III), insulin (Group IV), low and high doses of AgNPs (Groups V and VI), and their combinations with insulin (Groups VII–IX) markedly reduced *TCF7L2* expression compared to the diabetic group, with values approaching those of the control group. These findings suggest that diabetes induces an elevation in *TCF7L2* expression, whereas therapeutic interventions including extract, insulin, AgNPs and their combinations help in normalizing its expression.

Hematology: The hematological analysis revealed marked alterations in diabetic mice compared with controls, including elevated WBCs, platelet counts and significant reductions in RBCs, HB, HCT, MCV and MCH values, while MCHC abnormally increased (Table 4). Treatments with *T. indica* extract, insulin, and both low- and high-dose AgNPs improved most parameters, with combination therapies restoring values close to normal. Notably, AgNPs, particularly in high doses or when combined with insulin, were highly effective in normalizing RBC, Hb, WBCs, platelet counts and MCHC as compared to control levels. These findings indicate that green synthesized AgNPs, alone or combined with insulin or *T. indica* extract, exert significant protective and restorative effects on hematological parameters disrupted by diabetes.

Histology

Histological Examination of Pancreas: In the control group, the pancreas showed a well-defined intralobular duct, clearly visible acini, prominent and intact islets of Langerhans and uniform cytoplasmic distribution (Fig. 9). In the untreated diabetic group, histological analysis revealed a dilated duct, damaged acini, disrupted islets of Langerhans with poorly defined boundaries, and abnormal cytoplasmic distribution. Treatment with *T. indica* extract showed little improvement in islet structure, cytoplasmic organization, or boundary definition. Diabetic mice administered a low dose of AgNPs exhibited slight recovery in cytoplasmic distribution, boundary clarity, and structural organization. In contrast, those treated with a high dose of green synthesized AgNPs showed marked improvements, including restored islet morphology and a

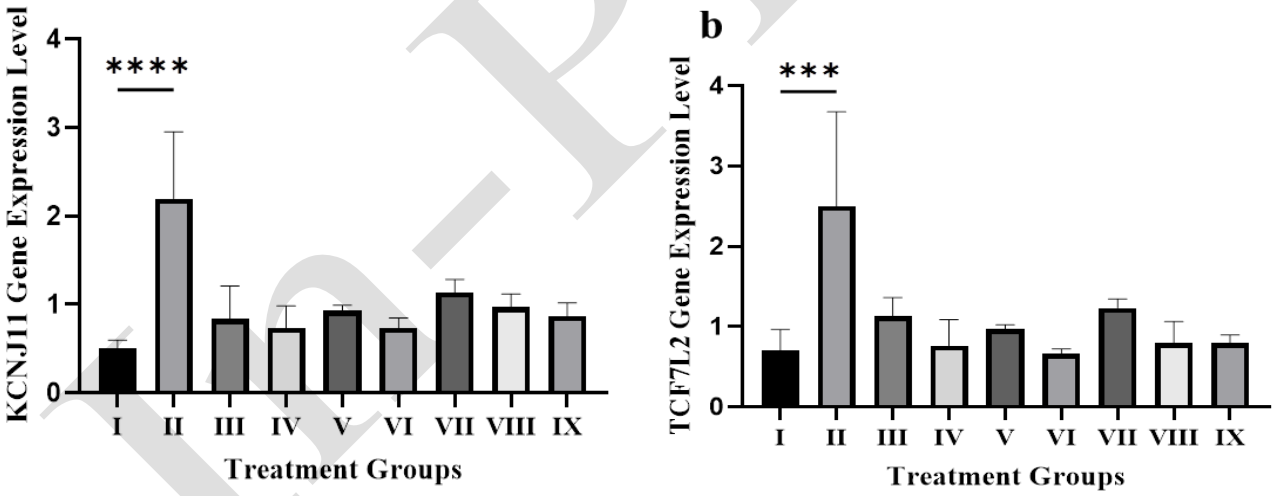

Fig. 8: *KCNJ11* and *TCF7L2* gene expression in diabetic mice. Asterisks indicate (One-way ANOVA, ***P<0.001, ****P<0.0001) significant difference. Group I: Control; Group II: Diabetic; Group III: Diabetic+Extract; Group IV: Diabetic+Insulin; Group V: Diabetic+Low dose of AgNPs; Group VI: Diabetic+High dose of AgNPs; Group VII: Diabetic+Low dose of AgNPs+ Insulin; Group VIII: Diabetic+High dose of AgNPs+ Insulin; Group IX: Diabetic +Insulin+ Extract.

Table 4: Impact of various treatments on the hematological parameters of albino mice in antidiabetic activity

Group	Treatment	WBCs(TLC) (10^3/μL)	Total RBCs (10^6/μL)	Hb (g/dL)	HCT(PVC) (%)	MCV (fL)	MCH (pg)	MCHC (g/dL)	Platelets (103/μL)
I	Control	4.63±0.08	7.8±0.05	12.83±0.21	53±0.57	65.6±0.33	24.3±0.88	27±1	464±0.33
II	Diabetic	6.93±0.23	4.3±0.20	8±0.57	36±0.56	47.3±1.20	15.3±1.45	36.6±0.66	934±0.57
III	Diabetic+Extract	5.43±0.22	5.26±0.40	11.83±0.72	47.3±1.45	50±0.57	22±0.57	24±0.57	616±21.8
IV	Diabetic+Insulin	5.6±3.2	5.40±0.20	11.43±0.92	45.6±0.66	53.6±1.85	19.3±0.88	25±1.15	664±3.60
V	Diabetic+Low dose of AgNPs	5.63±0.21	6.30±0.05	10.7±0.62	46.3±2.18	57.3±1.20	25.6±0.57	25.6±0.33	625±4.37
VI	Diabetic+High dose of AgNPs	4.9±0.11	6.8±0.15	13.67±0.35	46.6±0.88	56.3±2.18	20.6±0.88	22.3±2.02	462±9.025
VII	Diabetic+Low dose of AgNPs+ Insulin	4.83±0.12	6.8±0.05	10±1.15	50±0.57	62.3±1.86	23±0.57	27.2±0.41	613±9.07
VIII	Diabetic+High dose of AgNPs+ Insulin	4.56±0.22	6.16±0.12	12±0.57	48.23±0.66	61±0.57	22.3±0.87	28±0.57	462±9.02
IX	Diabetic+Insulin+Extract	4.93±0.176	6.26±0.13	12.10+0.32	47.6±0.66	60.3±0.88	20.3±0.66	24.3±1.45	664±1.66

* All the values are given as Mean ± SD.

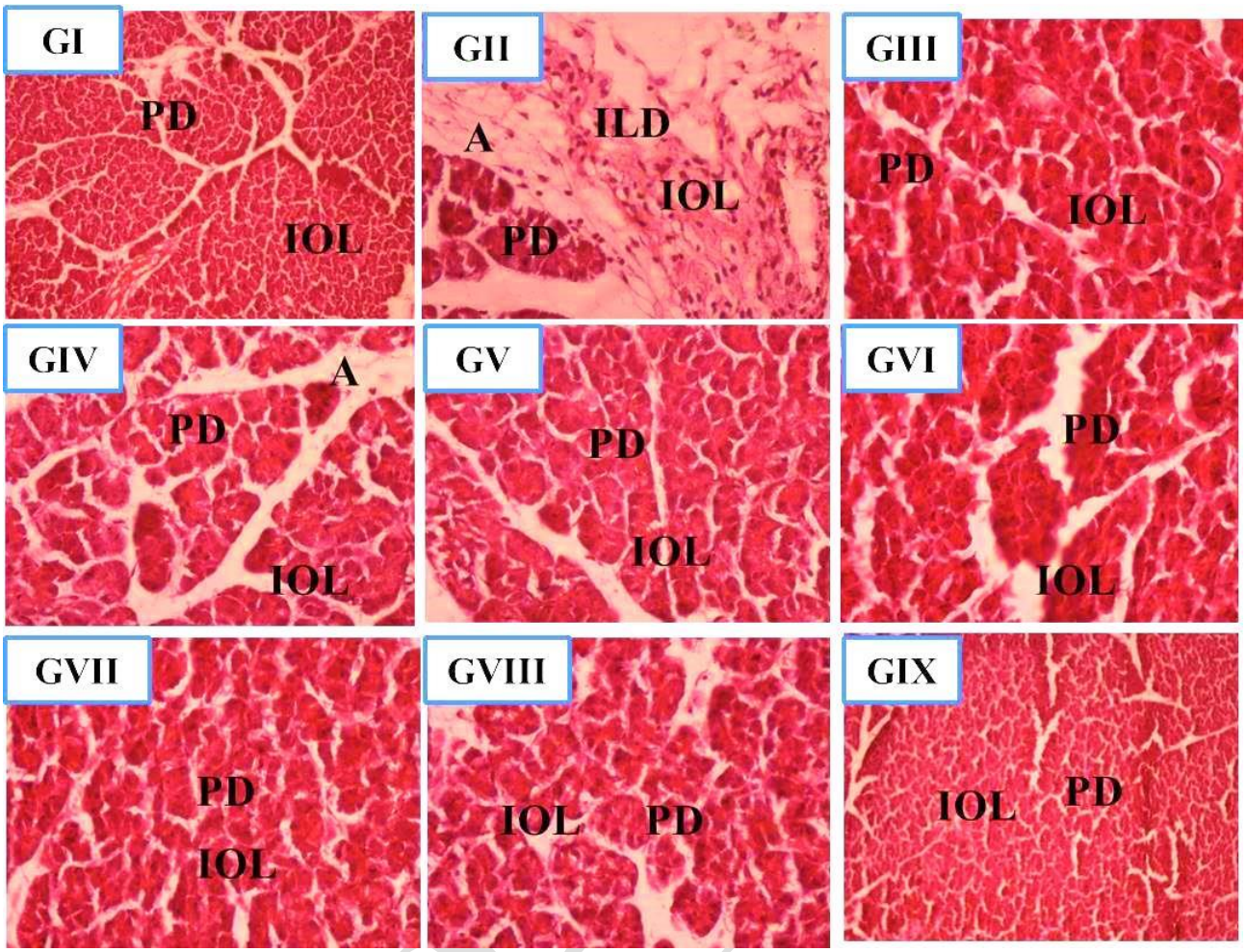

Fig. 9: Histological examination of pancreatic tissue of male albino mice. Group I: Control; Group II: Diabetic; Group III: Diabetic + Extract; Group IV: Diabetic + Insulin; Group V: Diabetic + Low dose of AgNPs; Group VI: Diabetic + High dose of AgNPs; Group VII: Diabetic + Low dose of AgNPs+ Insulin; Group VIII: Diabetic + High dose of AgNPs+ Insulin; Group IX: Diabetic +Insulin+ Extract. PD (pancreatic duct), IOL (islets of Langerhans), A (acini), ILD (intralobular duct), ICD (intercalated duct), ID (interlobular duct). 40X, Magnification.

clearer pancreatic duct. Minimal structural recovery observed in diabetic mice receiving the standard drug alone. However, animals treated with a combination of low-dose AgNPs and the drug demonstrated notable improvements in cytoplasmic distribution and islet morphology. Remarkably, diabetic mice treated with a high dose of AgNPs in combination with the drug exhibited pancreatic architecture closely resembling that of the control group.

DISCUSSION

DM is a severe metabolic disorder characterized by elevated blood glucose levels, if not properly managed, can lead to multiple chronic complications. The pancreas plays a central role in monitoring blood sugar levels and releasing insulin as needed. Researchers are seeking more natural therapeutic resources that can modulate glucose level without toxic side effects. Green synthesized AgNPs are gaining attention in nanomedicine with their ability to enhance medicinal properties (Rodrigues *et al*., 2017).

In this study AgNPs were prepared by reducing *T. Indica* leaf extract with $AgNO_3$ and the confirmation of AgNP formation achieved through a visible change in the color of the solution from yellow to brown (Asimuddin *et al*., 2020). Plant biomolecules were reduced by silver ions to produce metallic silver (Ag^-) from Ag^+ and were catalyzed by employing hydroxyl groups (–OH) of phytochemicals in order to create nucleation and nanoparticles (Košpić *et al*., 2022; Kurmi *et al*., 2022; Chinnasamy *et al*., 2021). Characterization of the synthesized nanoparticles using UV, FTIR, SEM, XRD, and EDX validated both their synthesis and coupling with phytochemicals, in line with earlier research findings (Tahir *et al.,* 2020; Chinnasamy *et al*., 2021; Ali *et al*., 2023; Mumtaz *et al*., 2023; Akhtar *et al*., 2024). These methods also validated the crystal morphology and structure of the nanoparticles and thus repeated the effectiveness of the synthesis process (Mumtaz *et al*., 2023; Subhani *et al*., 2023; Summer *et al.*, 2023; Mughal *et al*., 2024).

Based on the DPPH scavenging assay, the green synthesized AgNPs demonstrated strong antioxidant potential, capable of neutralizing free radicals by donating a hydrogen atom to stabilize the unpaired electron. This mechanism effectively reduces the reactivity of free radicals. Our findings align with those of Liu *et al*. (2020), who reported that radical scavenging activity is concentration-dependent, with higher nanoparticle concentrations leading to enhanced antioxidant effects. Elevated levels of ROS contribute to oxidative stress within cells, ultimately resulting in cell death (Li *et al*., 2020). Plant-derived

polyphenolic compounds, known for their potent antioxidant properties, play a protective role in preventing oxidative damage caused by free radicals (Kumari *et al*., 2022).

For biological assessment AgNPs, diabetic mice were grouped into nine sets. High dose AgNPs and conjugated AgNP-extract groups showed better body weight and blood glucose restoration as compared other groups. Haq *et al*. (2023) described the same restoration by *Penicillium niveum* extract-mediated AgNPs (Manam and Murugesan, 2021).

Most previous research has focused on evaluating the antioxidant, anti-inflammatory, hypoglycaemic, and histopathological effects of green-synthesised AgNPs, without extending to molecular or genetic pathways related to insulin regulation and glucose metabolism. For instance, studies using Moringa oleifera (Kumar *et al*., 2022), *Azadirachta indica* (Ibrahim *et al*., 2023), *Punica granatum* (Hussain *et al*., 2021), and *Zingiber officinale* (El-Deeb *et al*., 2020) demonstrated significant improvements in blood glucose, insulin levels, and pancreatic tissue restoration. However none of these studies investigated *KCNJ11* or *TCF7L2* gene expression. The current study uniquely contributes to the literature by examining how plant-mediated AgNPs affect these genes, which are key regulators of insulin secretion and β-cell function.

By targeting these two genes, our study aims to fill a critical gap in nanomedicine-based diabetes research. While prior works have validated the therapeutic efficacy of plant-based nanoparticles, the molecular mechanisms governing these effects remain insufficiently understood. Investigating *KCNJ11* and *TCF7L2* expression provides a mechanistic link between green-synthesised AgNP treatment and glucose regulation at the gene level, thereby enhancing the scientific contribution of this research as *KCNJ11* encodes the Kir6.2 protein that regulates insulin release through ATP-sensitive potassium channels, while *TCF7L2* encodes the TCF4 transcription factor involved in Wnt signaling and glucose metabolism.

In current study *KCNJ11* mRNA significantly upregulated in the diabetic group (Group II) and diabetic treated groups returned toward control levels after treatment with the plant extract, insulin, AgNPs and their combinations. Our findings are consistent with Romo-Robles *et al*. (2020), who demonstrated that plant extracts and antioxidant supplementation modulate ion-channel expression in diabetic rodents. Antioxidant interventions were shown to alter *KCNJ11* expression by reducing oxidative stress, enhancing mitochondrial function and regulating transcriptional pathways. These mechanisms support our observation that plant extract treatment normalized *KCNJ11* expression in diabetic mice. This regulation suggests a restoration of β-cell function and insulin secretory capacity (Ashcroft and Rorsman, 2018). In diabetes, oxidative stress and glucotoxicity impair $KATP_{ATP}$ channel expression and function, leading to dysregulated insulin release (Taneera *et al*., 2019).

Our findings of *TCF7L2* gene expression in diabetic mice concur with previous research by Lyssenko *et al*. (2007). The results are similar the findings of Abozaid *et al*. (2023), who reported that diabetic animals treated with chitosan-encapsulated selenium nanoparticles combined with glibenclamide showed a significant ($P<0.05$) decrease in *TCF7L2* gene expression. *TCF7L2* is a major regulator of blood glucose homeostasis, whose product is a transcription factor in the developing pancreas and is involved in the Wnt signaling pathway through glucagon-like peptides (GLPs). Genetic variations of *TFC7L2* can cause insulin resistance through impaired GLP-1 function. Verma *et al*. (2020) further observed that genetic variation in this gene enhances the risk for T2DM through modulation of insulin secretion. *TCF7L2* overexpression could also interfere with pancreatic β-cell dysfunction (Lyssenko *et al*., 2007; Jin, 2022).

The WBC count significantly ($P<0.05$) higher in the untreated diabetic group than in the non-diabetic group and the extract-treated groups. The finding also shows that treatment with high concentrations of AgNPs resulted in significant improvements of Hb, RBCs and platelets compared to the diabetic untreated and the non-diabetic group. These findings concur with Iyare and Obaji (2014) findings, where *Azadirachta indica* found to be a hematopoietic agent that can boost blood parameters. The increase in blood component observed can be attributed to the bioactive compounds with flavonoids and quercetin, and these possess hematopoietic activities (Raja *et al*., 2011).

Histopathological analysis of the pancreas showed that *T. indica*-AgNPs caused more effective islet cell regeneration and recovery of β-cells than synthetic drugs. B-cell mass enhanced and oxidative injury reduced, in AgNPs-treated mice relative to untreated diabetic controls. This suggests that AgNPs may be maintaining β-cells safe from reactive oxygen species-induced apoptosis (Pan *et al*., 2022). Similar findings were reported by Wahab *et al*. (2022) and Ullah *et al*. (2021) who established the increased regenerative capacity of green-synthesized AgNPs when compared to conventional therapies.

Conclusions: The outcome of the current study indicated that AgNPs synthesis using the leaf extract of *T. indica* is a low-cost, simple and eco-friendly process. The SEM examination confirmed that most of the NPs were crystalline in shape. FTIR spectroscopy also validated the occurrence of flavonoids and polyphenols of the extract being conjugated with the AgNPs, indicating that they play a role in stabilizing the nanoparticles. Therapeutic potential of these NPs green synthesized, particularly their antioxidant and antidiabetic potential had been evaluated. The result showed that dysregulation of *KCNJ11* and *TCF7L2* observed in diabetic mice underscores their critical role in β-cell function and glucose regulation, while therapeutic interventions effectively restored their expression toward normal levels. The results show that AgNPs purified from *T. indica* possess robust antidiabetic potency and can provide an inexpensive means of managing diabetes. The present findings show that green synthesized AgNPs are potent effective antioxidant and antidiabetic compounds and may be valuable tools in designing pharmacological and therapeutic approaches toward diabetes and other metabolic dysfunctions.

Author Contributions: Conceptualization; SI, FR, SS, Formal analysis; SI, FR, IN, AE, SN, FY, Supervision; FR, Project administration; SI.

REFERENCES

Abozaid OA, El-Sonbaty SM, Hamam NM, *et al*., 2023. Chitosan-encapsulated nano-selenium targeting *TCF7L2*, *PPARγ*, and *CAPN10* genes in diabetic rats. Biol Trace Elem Res 201(1): 306-323.

Akhtar MF, Irshad M, Ali S, *et al*., 2024. Spectrophotometric, microscopic, crystallographic and X-ray based optimization and biological applications of *Olea paniculata* leaf extract mediated silver nanoparticles. S Afr J Bot 166:97–105.

Ali F, Ali S, Shahbaz S, *et al*., 2023. Bactericidal and antioxidant potential of Moringa oleifera capped silver nanoparticles under varied conditions. Chemistry Select 8:e202301889.

Ashcroft FM, Rorsman P, 2018. *KATP channels and islet function in health and disease. Diabetologia 61(*2): 213–223.

Asimuddin M, Shaik MR, Adil SF, *et al*., 2020. *Azadirachta indica* based biosynthesis of silver nanoparticles and evaluation of their antibacterial and cytotoxic effects. J King Saud Univ Sci 32:648–656.

Banerjee P, Satapathy M, Mukhopahayay A, *et al*., 2014. Leaf extract mediated green synthesis of silver nanoparticles from widely available Indian plants: synthesis, characterization, antimicrobial property and toxicity analysis. Bioresour Bioprocess 1:3.

Barroso, I., Luan, J. A., Middelberg, *et al*., 2003. Candidate gene association study in type 2 diabetes indicates a role for genes involved in β-cell function as well as insulin action. *PLoS biology*, *1*(1), e20.

Begum S, Rana S, Shabir N, Rani S, 2022. Recent advances in green synthesis, characterization, and applications of bioactive metallic nanoparticles. Pharmaceuticals 15(4):455

Chinnasamy G, Chandrasekharan S, Koh TW, *et al*., 2021. Synthesis, characterization, antibacterial and wound healing efficacy of silver nanoparticles from *Azadirachta indica*. Front Microbiol 12:611560.

Chopra H, Bibi S, Kumar S, *et al*., 2022. Green metallic nanoparticles: Biosynthesis to applications. Front Bioeng Biotechnol 10:874742.

Elumalai D, Hemavathi M, Deepaa CV, *et al*., 2017. Evaluation of phytosynthesised silver nanoparticles from leaf extracts of *Leucas aspe*ra and *Hyptis suaveolens* and their larvicidal activity against malaria, dengue and filariasis vectors. Parasite Epidemiol Control 2:15–26.

El-Deeb NM, Salem SS and Elzainy AR, 2020. Green synthesis of silver nanoparticles using *Zingiber officinale* extract and their potent antioxidant and antidiabetic activities. Journal of Drug Delivery Science and Technology, 60, 102020.

Fischer AH, Jacobson KA, Rose J, *et al*., 2008. Hematoxylin and eosin staining of tissue and cell sections. Cold Spring Harb Protoc 5:4986.

Garg S, Muangman T, Huifu H, *et al*., 2018. Bioactivities in the tamarind seed extracts: a preliminary study. AIP Conf Proc 020018.

Hussain A, Ali S and Rehman T, 2021. Biogenic synthesis of silver nanoparticles using *Punica granatum* peel extract and evaluation of their biological activities. Materials Today: Proceedings, 45, 3501–3507.

Haq MNU, Shah GM, Menaa F, *et al*., 2023. Green silver nanoparticles synthesized from *Taverniera couneifolia* elicits effective anti-diabetic effect in alloxan-induced diabetic Wistar rats. Nanomaterials 12:1035–1047.

Iyare E, Obaji NN, 2014. Effects of aqueous leaf extract of *Azadirachta indica* on some haematological parameters and blood glucose level in female rats. Niger J Exp Clin Biosci 2:54–58.

Ibrahim, H. M., Ahmed, M. A., and El-Moslamy, S. H. 2023. Green synthesis of silver nanoparticles using *Azadirachta indica* leaf extract and their antioxidant and antidiabetic activities. Journal of Applied Nanoscience, 13(2), 345–358.

Jaffar SS, Saallah S, Misson M, *et al*., 2023. Green synthesis of flower-like carrageenan-silver nanoparticles and elucidation of its physicochemical and antibacterial properties. Molecules 28:907.

Jin, T. 2022. *Mechanistic insights into TCF7L2 and Wnt signaling in β-cell biology and diabetes*. *Front. in Endocr. 13*: 828420.

Komutarin T, Azadi S, Butterworth L, *et al*., 2004. Extract of the seed coat of *Tamarindus indica* inhibits nitric oxide production by murine macrophages *in vitro* and *in vivo*. Food Chem Toxicol 42:649–658.

Kumar, S., Singh, P., and Verma, R. 2022. Green synthesis of silver nanoparticles using *Moringa oleifera* and their evaluation for antioxidant, anti-inflammatory, and antidiabetic potential. Journal of Nanobiotechnology, 20(1), 145.

Košpić K, Biba R, Peharec Štefanić P, *et al*., 2022. Silver nanoparticle effects on antioxidant response in tobacco are modulated by surface coating. Plants 11:2402.

Kumari SA, Patlolla AK, Madhusudhanachary P, 2022. Biosynthesis of silver nanoparticles using *Azadirachta indica* and their antioxidant and anticancer effects in cell lines. Micromachines 13:1416.

Kurmi UG, Zahir A, Musa A, *et al*., 2022. Review of Nigerian medicinal plants used in the management of diabetes mellitus. J Clin Med Images Case Rep 2:1–5.

Kuru P, 2014. *Tamarindus indica* and its health related effects. Asian Pac J Trop Biomed 4:676–681.

Li R, Ou J, Li L, Yang Y, Zhao J, Wu R. 2019. The Wnt signaling pathway effector *TCF7L2* mediates olanzapine-induced weight gain and insulin resistance. Front Pharmacol 9:379.

Li Y, Li N, Jiang W, *et al*., 2020. In situ decorated Au NPs on pectin-modified Fe3O4 NPs as a novel magnetic nanocomposite (Fe_3O_4/Pectin/Au) for catalytic reduction of nitroarenes and investigation of its anti-human lung cancer activities. Int J Biol Macromol 163:2162–2171.

Liu J, Zangeneh A, Zangeneh MM, *et al*., 2020. Antioxidant, cytotoxicity, anti-human esophageal squamous cell carcinoma, anti-human Caucasian esophageal carcinoma, anti-adenocarcinoma of the gastroesophageal junction, and anti-distal esophageal adenocarcinoma properties of gold nanoparticles green synthesized by *Rhus coriaria* L. fruit aqueous extract. J Exp Nanosci 15:202–216.

Lyssenko V, Lupi R, Marchetti P, *et al*., 2007. Mechanisms by which common variants in the *TCF7L2* gene increase risk of type 2 diabetes. The Journal of clinical investigation, 117(8): 2155-2163.

Manam VK, Murugesan S, 2021. Anti-diabetic efficacy of silver nanoparticles biosynthesized from marine red seaweed Halymenia porphyroides Boergesen on alloxan stimulated hyperglycemic activity in rats. Int J Pharm Sci Nanotechnol 14:5639–5646.

Menati L, Meisami A, Zarebavani M, 2020. The potential effects of dietary flavones on diabetic nephropathy: a review of mechanisms. J Renal Inj Prev 9:09.

Mughal TA, Ali S, Mumtaz S, *et al*., 2024. Evaluating the biological (antidiabetic) potential of TEM, FTIR, XRD, and UV-spectra observed *Berberis lyceum* conjugated silver nanoparticles. Microsc Res Tech 87:1286–1305.

Mumtaz S, Ali S, Kazmi SAR, *et al*., 2023. Analysis of the antimicrobial potential of sericin-coated silver nanoparticles against human pathogens. Microsc Res Tech 86:320–330.

Mumtaz S, Ali S, Tahir HM, *et al*., 2023. Biological applications of biogenic silk fibroin–chitosan blend zinc oxide nanoparticles. Polym Bull 81:2933–2956.

Pan Y, Yuan S, Teng Y, *et al*., 2022. Antioxidation of a proteoglycan from Ganoderma lucidum protects pancreatic β-cells against oxidative stress-induced apoptosis *in vitro* and *in vivo*. Int J Biol Macromol 200:470–486.

Rahuman HBH, Dhandapani R, Narayanan S, *et al*., 2022. Medicinal plants mediated the green synthesis of silver nanoparticles and their biomedical applications. IET Nanobiotechnol 16:115–144.

Raja SB, Murali MR, Kumar NK, *et al*., 2011. Isolation and partial characterisation of a novel lectin from *Aegle marmelos* fruit and its effect on adherence and invasion of Shigellae to HT29 cells. PLoS One 6:e16231.

Rio DC, Ares M, Hannon GJ, Nilsen TW. 2010. Purification of RNA using TRIzol (TRI reagent). Cold Spring Harbor Protoc 6:5439.

Rodrigues MJ, Custódio L, Lopes A, *et al*., 2017. Unlocking the *in vitro* anti-inflammatory and antidiabetic potential of Polygonum maritimum. Pharm Biol 55:1348–1357.

Romo-Robles DP, Domínguez-Avila JA, Montiel-Herrera M, et al., 2020. Effects of a Diet Supplemented with Fruit Antioxidants (Mango) on the Expression of Kir6.2 (*KCNJ11*) in the Hippocampus and Kidney of Diabetic Rats. Neurophysiology 52(6): 430-437.

Sabapathi N, Ramalingam S, Aruljothi KN, *et al*., 2023. Characterization and therapeutic applications of biosynthesized silver nanoparticles using *Cassia auriculata* flower extract. Plants 12:707.

Saratale RG, Shin HS, Kumar G, *et al*., 2018. Exploiting antidiabetic activity of silver nanoparticles synthesized using Punica granatum leaves and anticancer potential against human liver cancer cells (HepG2). Artif Cells Nanomed Biotechnol 46:211-222.

Subhani AA, Irshad M, Ali S, *et al*., 2023. UV-spectrophotometric optimization of temperature, pH, concentration and time for *Eucalyptus globulus* capped silver nanoparticles synthesis, their characterization and evaluation of biological applications. J Fluoresc 34:655.

Summer M, Ali S, Tahir HM, *et al*., 2023. Silk sericin protein: turning discarded biopolymer into ecofriendly and valuable reducing, capping and stabilizing agent for nanoparticles synthesis using sonication. Macromol Chem Phys 224:2300124.

Tahir H, Rashid F, Ali S, *et al*., 2023. Spectrophotometrically, spectroscopically, microscopically and thermogravimetrically optimized TiO_2 and ZnO nanoparticles and their bactericidal, antioxidant and cytotoxic potential: a novel comparative approach. J Fluoresc 1–15.

Tahir M, Saleem F, Ali S, *et al*., 2020. Synthesis of sericin-conjugated silver nanoparticles and their potential antimicrobial activity. J Basic Microbiol 60:458–467.

Taneera J, *et al*., 2019. *Regulation of KCNJ11 expression and β-cell function under oxidative stress*. *J Molecul Endocrinol 63*(3):221-233.

Ullah S, Shah SWA, Qureshi MT, *et al*., 2021. Antidiabetic and hypolipidemic potential of green AgNPs against diabetic mice. ACS Appl Bio Mater 4:3433-3442.

Verma AK, Beg MMA, Saleem M, *et al*., 2020. Cell free *TCF7L2* gene alteration and their association with Type 2 diabetes mellitus in North Indian population. Meta Gene 25:100727.

Wahab M, Bhatti A, John P, 2022. Evaluation of antidiabetic activity of biogenic silver nanoparticles using *Thymus serpyllum* on streptozotocin-induced diabetic BALB/c mice. Polymers 14:3138.